Desalination and Water Treatment
www.deswater.com

doi: 10.5004/dwt.2017.20318

70 (2017) 250–260
April

Application of molybdenum disulfide nanosheets for adsorption of tetracycline in water samples

Mohammad Javad Aghagoli[a], Farzaneh Shemirani[b,*]

[a]*Wellbeing of the work research center, Qom university of medical sciences and health services, School of Chemistry, University College of Science, University of Tehran, P.O. Box 14155-6455, Tehran, Iran, email: j.aghagoli@ut.ac.ir (M.J. Aghagoli)*
[b]*Department of Analytical Chemistry, University College of Science, University of Tehran, P.O. Box 14155-6455, Tehran, Iran, email: shemiran@khayam.ut.ac.ir (F. Shemirani)*

Received 1 June 2016; Accepted 29 October 2016

ABSTRACT

Molybdenum disulfide (MoS_2) is a layered material with unique two-dimensional structure which has abundant electron density on edges and surfaces. These adsorption sites could interact with polycyclic aromatic compounds by π–π stacking. Therefore, MoS_2 nanosheets will no longer be modified or functionalized. In this study, MoS_2 nanosheets were prepared by a simple and low cost hydrothermal method, and characterized by using different techniques, such as field emission scanning electron microscopy, transmission electron microscopy, X-ray power diffraction, and energy dispersive X-ray. The resultant MoS_2 nanosheets were applied for preconcentration of tetracycline (TC) as a model analyte in solid-phase extraction. Various experimental parameters (pH, adsorbent amount, contact time, type and volume of eluent and desorption time, sample volume, salt addition, interferences, and reusability) affecting the extraction process were studied. Under optimum conditions, the calibration graph was linear in the concentration range of 0.025–5 mg L^{-1} with a detection limit of 7.91 μg L^{-1}. The relative standard deviation values of the method were 3.3%. The reusability (five consecutive cycles) and adsorption capacity (57.47 mg g^{-1}) of MoS_2 nanostructures were favorable. The proposed method was successfully applied to the TC analysis in real samples, such as fish pond water, agriculture-influenced water, and river water. Good spiked recoveries over the range of 92.0%–103.0% were obtained.

Keywords: MoS_2 nanosheets; Tetracycline preconcentration; Real samples

1. Introduction

Environmental pollutants produced by the mass productions and great usages of pharmaceutical antibiotics have attracted increasing concern in recent years [1]. Antibiotics are widely used as infectious disease medicines, which have become a serious problem as they have variety of potential adverse effects, including acute toxicity, impact on photosynthetic organisms, disruption of natural microbial populations, and dissemination into antibiotic resistant genes among microorganisms [2]. Among various antibiotics, tetracycline (TC) has been widely used in human and veterinary medicine and gradually become the second most widely used antibiotic in the world [3]. TC has a high aqueous solubility with a long environmental half-life [4] and has been shown to disrupt microbial soil respiration [5], Fe(III) reduction [6], and nitrification [7]. TC is difficult to be metabolized and absorbed by the treated humans and animals; consequently, large fractions are excreted through urine and feces as unmodified parent compound [8]. TC has been determined in a number of samples, such as milk [9], plasma [10], pharmaceutical products [11], and water [12]. So far, various adsorbents including palygorskite [13], multi-walled carbon nanotubes [14], aluminum and iron hydrous oxides [15], graphene oxide [16], silica [17], smectite clay [18], montmorillonite [19], chitosan particles [20], aluminum oxide [21],

* Corresponding author.

activated carbon [22], diatomite [23], polystyrene resins [24], boron nitride [25], metal ions impregnated polystyrene resins [26], Cu-13X [27], and molecularly imprinted polymer [28] have been studied for adsorption of pharmaceutical antibiotics from foods, conventional waters, and wastewaters.

In the last decades, the layered transition metal dichalcogenides (TMDs) with the generic formula MX_2 where M represents transition metals, such as molybdenum (Mo), tungsten (W), titanium (Ti), zirconium (Zr), or hafnium (Hf) and X represents chalcogens, such as sulfur (S), selenium (Se), or tellurium (Te) have attracted much interest. Molybdenum disulfide (MoS_2), a typical of TMD, was first synthesized by Hershfinkel et al. [29] via the gas-phase reaction between molybdenum trioxide (MoO_3) and H_2S in a reducing atmosphere at elevated temperature (800°C–1,000°C). MoS_2 has layered structure that the monolayer consists of transition-metal atoms surrounded in a sandwich structure by chalcogenide atoms, which are covalently bonded to the transition-metal atoms [30]. However, the interactions between the individual monolayers are of the van der Waals type.

Many methods, such as microwave plasma, CO_2 laser irradiation, radio frequency sputtering, pulsed laser evaporation, chemical vapor transport, and metal organic vapor deposition, have been employed for the synthesis of MoS_2 nanostructures [31]. However, these methods, either involve a high temperature procedure or a complicated manipulation, which may lead to the cost increase and further limit the potential applications. The hydrothermal method is considered as one of the promising routes, owing to its advantages of environment friendly, simple fabrication process, and high product purity [32]. Thus, hydrothermal method was selected for the synthesis of adsorbent.

There have been many studies on MoS_2, due to the suitable properties for diversity of applications, such as electronic devices [33], lithium ion batteries [34], optical identification [35], and sensing and biosensing [36]. Also, MoS_2 shows excellent properties, such as catalysis, intercalation, lubrication, anisotropy, chemically inertness, and photocorrosion resistance [31]. Study of former researches indicated that adsorption performance of MoS_2 was investigated in materials removal, such as aromatic sulfur compounds in fuels, doxycycline pharmaceutical, and organic dyes in aqueous solution [37–39]. However, the MoS_2 nanosheets have not been employed as adsorbent of TC by solid-phase separation (SPE) system in analytical work in the presence of different foreign species till now. Appropriate adsorption features of synthesized MoS_2 are related to the edges and surfaces of electron rich which made it as an appropriate candidate for the adsorption of polycyclic aromatic compounds like TC. It should be noted that MoS_2 has been considered to be as an environmentally friendly and chemically inert compound [40].

In this research, MoS_2 nanosheets were structurally synthesized and morphologically characterized and used for the preconcentration of TC as a model analyte. Our proposed adsorbent has several attractive features compared with previous adsorbents including novelty, needless to pretreatment steps (such as modification and functionalization), numerous adsorption sites in edges and surface of each sheet, low cost synthesis, reusability and high recovery, environmentally friendly, and chemically inert [40] which made it as an appropriate candidate for the adsorption of polycyclic aromatic compounds via π–π interaction between analyte and MoS_2.

The effect of various experimental parameters on the adsorption of antibiotic was investigated in batch adsorption experiments and the proposed method was successfully employed for the preconcentration of TC in real samples, such as fish pond water, agriculture-influenced water, and river water.

2. Experimental

2.2. Materials and solutions

All chemicals used were of analytical reagent grade. TC (≥95% purity), MoO_3, potassium thiocyanate (KSCN), and sodium chloride were obtained from Sigma-Aldrich Chemical Co. (Milwaukee, WI, USA). TC stock solution and other solutions were prepared in distilled water. The pH of the solutions was adjusted by NaOH (0.1 mol L^{-1}) and followed by dropwise addition of HCl (0.1 mol L^{-1}). HNO_3 (65%), HCl (37%), and NaOH (Merck, Darmstadt, Germany) were tested as eluent. The glassware used were kept in acetone overnight and subsequently washed several times with double distilled deionized water before using.

2.2. Apparatus

A PerkinElmer (Lambda 25, PerkinElmer) spectrophotometer was used for UV–vis spectra acquisition. The pH-meter model 692 from Metrohm (Herisau, Switzerland) with combined glass electrode and a universal pH indicator (0–14) from Merck were used for the pH measurements. A universal 320R refrigerated centrifuge equipped with an angle rotor (6-place, 9,000 rpm, Cat. No. 1620A) was from Hettich (Kirchlengern, Germany). Surface morphology analysis of the adsorbents was carried out using a field emission scanning electron microscope (FESEM), model S-4160 (procurement, Japan). Also transmission electron microscopy (TEM) (Hitachi High-Technologies Europe GmbH, HF 2000, Germany) was used for characterization of the size of layer MoS_2. For X-ray power diffraction (XRD) measurements, a Shimadzu 7000 S X-ray diffract meter with Cu Kα radiation (λ = 1.54 Å) was used. Energy dispersive X-ray (EDX) was performed by Oxford ED-2000 (England).

2.3. Synthesis of MoS_2 nanosheets

The MoS_2 was prepared as described by Chao et al. [38]. Briefly, 5 mmol MoO_3, 12.5 mmol KSCN, and 60 mL of deionized water were mixture and put in 100 mL Teflon-coated autoclave at 453 K for 24 h by hydrothermal method. After cooling naturally, the black MoS_2 was washed with distilled water and absolute ethanol for several times and dried at 378 K for 10 h.

2.4. Sample collection and preparation

The samples were analyzed immediately after preparation. Fish pond water, agriculture-influenced water, and river water were got from farmlands (Var e olia village,

Mahallat, Iran). All of the collected water samples were filtered with filter paper, pH of the samples was adjusted to 4.5 and the general procedure was carried out. The analyte concentration in the real samples was determined by UV–vis spectrophotometry and HPLC.

2.5. General procedure

The batch experiments were carried out in 25 mL graduate falcon tubes containing the mixture of 10 mg adsorbent, 20% (w/v) NaCl, and 20 mL TC aqueous solution (200 μg L^{-1}) with pH of 4.5. Conical bottom tubes were wrapped in aluminum foil to avoid possible photodegradation of TC and were stirred for 60 min at ambient temperature in order to adsorption. After centrifuging of suspensions at 7,500 rpm for 15 min and supernatant was decanted, 2 mL of 2 mol L^{-1} HNO_3 was used for desorption of the TC which had remained on MoS_2 adsorbent (shaking time: 5 min; centrifuging: 5 min). The amount of TC in eluted of solution was measured by UV–vis spectrophotometer absorbance at 357.2 nm, using a calibration curve built with the antibiotics solution of different concentrations. The other adsorption experiments were performed under the same conditions.

3. Results and discussion

3.1. Characterization of MoS_2 nanostructures

FESEM, TEM, XRD, and EDX were employed to characterize MoS_2 nanostructures prepared by hydrothermal method. The FESEM characterization of the MoS_2 is reported in Fig. 1(A). This figure shows high degree of agglomeration and an average size of the sheets of flower like particles about 80 nm. A TEM image in Fig. 1(B) clearly shows that the MoS_2 layers are well stacked. Also, Fig. 1(B) reveals the formation of graphene-like structure, though the major parts of the images gives an impression for the presence of randomly oriented layers of MoS_2. The desultory parallel structure may be ascribed to the few-layered adsorbent stacked in agglomerates. The average interlayer distance is close to 0.65 nm, which corresponds to the *d* (002) spacing of the 2H-MoS_2 lattice fringe. The MoS_2 with a layer separation in the range of 0.65–0.69 nm reported in literature [41]. Fig. 1(C) showed the XRD pattern of the MoS_2, and the corresponding peak did not present the *d* (002) reflection, testifying the presence of a few layers of MoS_2 [41]. The other (100), (103), and (110) reflections could be readily indexed as hexagonal MoS_2 and were identical with the reported data in JCPDS card no. 37-1492 [42]. The EDX of

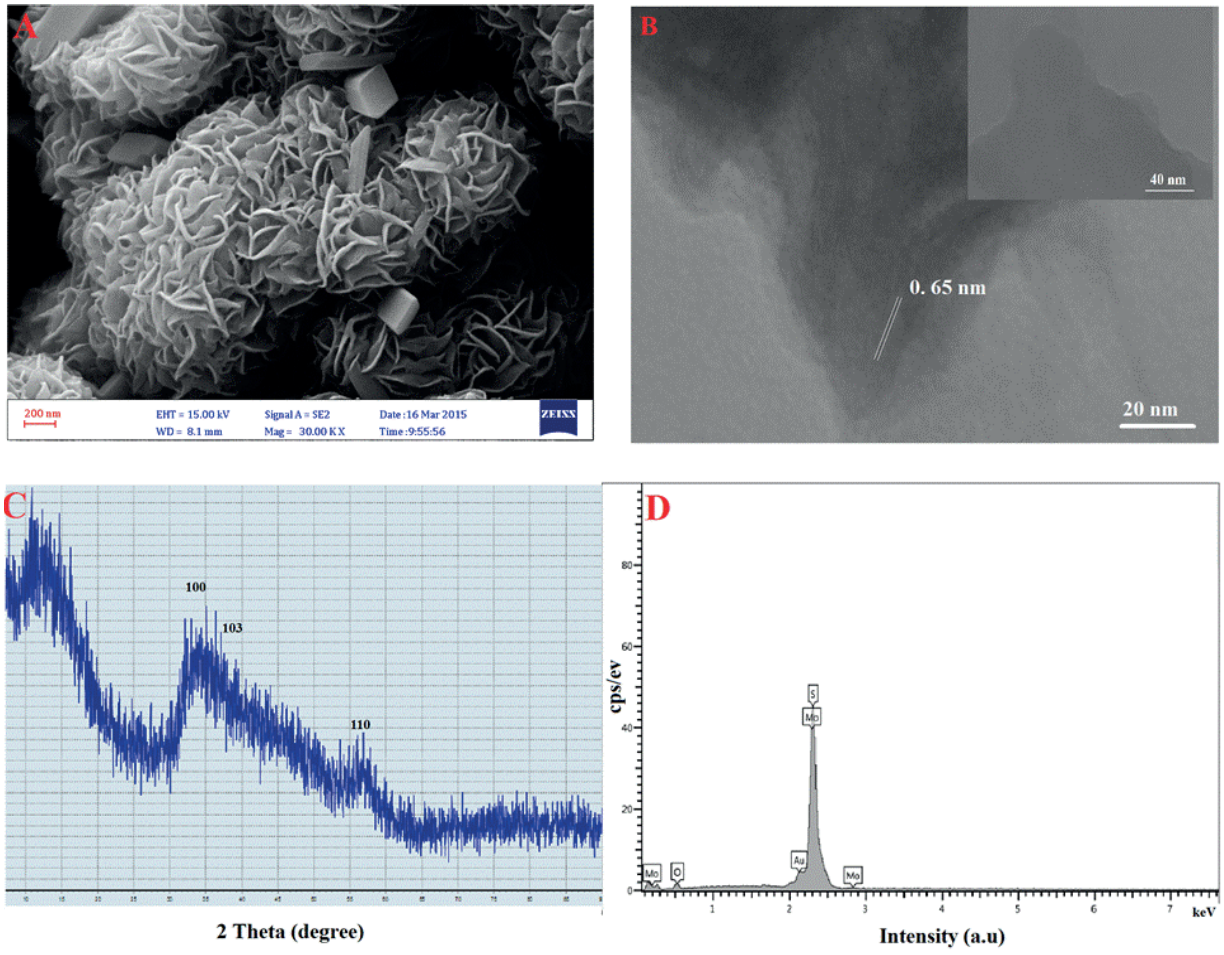

Fig. 1. (A) FESEM image of MoS_2 nanosheets, (B) the desultory parallel structure may be ascribed to the few-layered MoS_2 stacked in agglomerates, (C) XRD pattern of MoS_2, and (D) EDX image of MoS_2 nanosheets.

MoS_2 (Fig. 1(D)) has been analyzed, where the Mo and S were the main element in this material.

3.2. Optimizing the effective parameters in preconcentration

3.2.1. Effect of pH

The influence of solution pH on adsorption of TC onto MoS_2 was studied in the pH range of 2.0–8.0. The results were shown in Fig. 2(A). The recovery of TC increased when the pH increased from 2.0 to 4.5 and then decreased with further increasing pH from 6 to 8. This trend suggested that the adsorption of TC onto MoS_2 was strongly dependent on pH values and TC could be effectively recovered in a wide range of pH 4.0–4.5. According to the results recovery of the TC, pH of 4.5 was chosen.

The variation in pH can lead to a change in chemical speciation for ionizable organic compounds [43]. TC has several polar/ionizable groups, including amino, carboxyl, phenol, alcohol, and ketone. It has three acid dissociation constants (pK_a = 3.3, 7.7, and 9.7) and exists as a cationic, zwitterionic, and anionic species under acidic, moderately acidic to neutral, and alkaline conditions [44]. Specially, the amino group on the ring C_4 has pK_a of 9.7 and is easily protonated under favorable conditions. A π–π interaction as dominant driving force has always been used to explain the mechanism of aromatic adsorbate to MoS_2 surfaces [45]. MoS_2 as a layered nanomaterial displays a maximum adsorption at 357.2 nm due to its π–π transition. Moreover, as shown in Fig. 2(A), the obvious decline of the recovery as pH < 4.0 or pH > 6.0 indicated that electrostatic interactions between TC and the MoS_2 might also take place and affect the adsorption to a certain extent.

3.2.2. Effect of the adsorbent amount

The effect of the mass of the adsorbent on the adsorption of TC was studied by varying the amount of the adsorbent within the range of 5.0–20.0 mg. It was found that 10.0 mg of the prepared adsorbent is sufficient for the quantitative recovery of the antibiotic.

3.2.3. Effect of the contact time

Contact time between the MoS_2 and TC is also known as an important factor. The effect of shaking time was monitored by using the selected shaking time intervals 10–100 min and the antibiotic adsorption values were determined under the condition of pH 4.5. As the contact time increased,

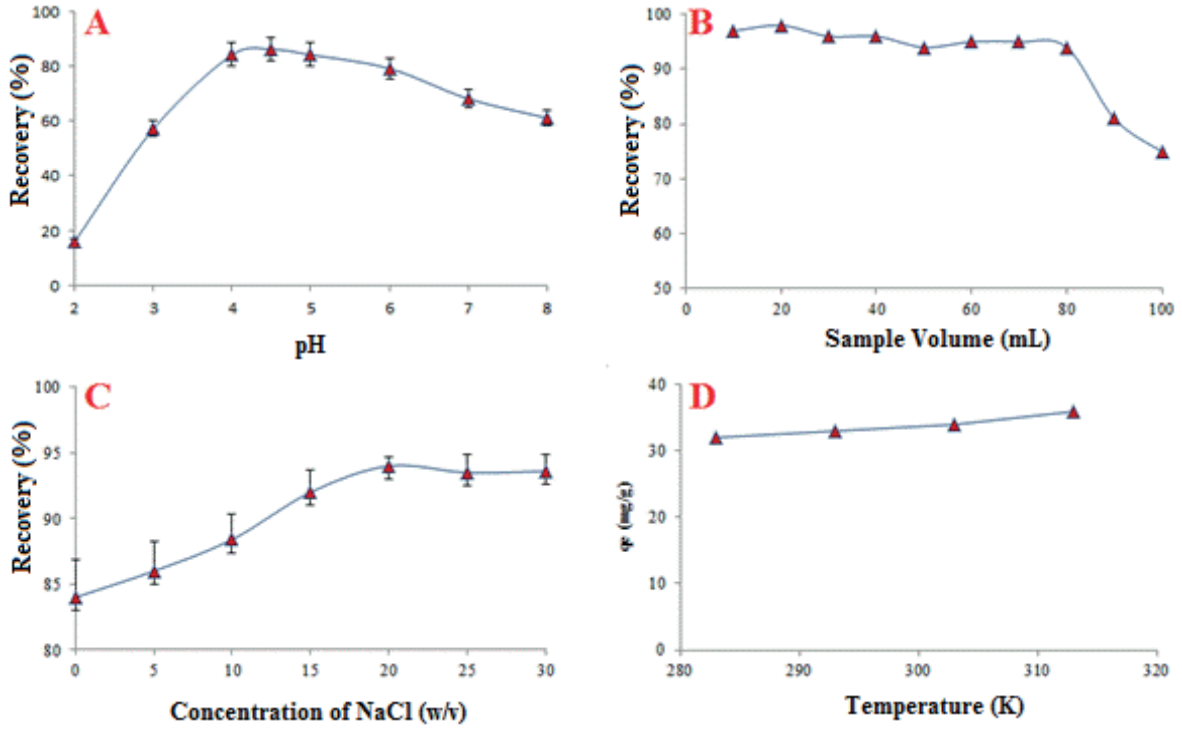

Fig. 2. (A) Effects of pH for TC adsorption onto MoS_2 nanosheets. Conditions: C_0: 200 μg L^{-1} of TC solution; mass of adsorbent: 10 mg; volume: 20 mL; contact time: 40 min; and eluent: 2.0 mL HNO_3 (1 mol L^{-1}). (B) Effects of ample volume for TC adsorption onto MoS_2 nanosheets. Conditions: C_0: 200 μg L^{-1} of TC solution; pH: 4.5; mass of adsorbent: 10 mg, contact time: 40 min; and the eluent: 2.0 mL HNO_3 (1 mol L^{-1}). (C) Effects of ionic strength (NaCl) for TC adsorption onto MoS_2 nanosheets. Conditions: C_0: 200 μg L^{-1} of TC solution; pH: 4.5; mass of adsorbent: 10 mg; volume: 20 mL; contact time: 40 min; and the eluent: 2.0 mL HNO_3 (1 mol L^{-1}). (D) Effects of temperature for TC adsorption onto MoS_2 nanosheets. Conditions: C_0: 200 μg L^{-1} of TC solution; pH: 4.5; mass of adsorbent: 10 mg; volume: 20 mL; ionic strength: 20% w/v; and contact time: 40 min.

the adsorption efficiency gradually increased and then remained nearly constant after 60 min. The results showed that the adsorption process should equilibrate for a sufficient time to achieve the high adsorption percentage. In the present work, 60 min was selected as the optimal adsorption time.

3.2.4. Desorption conditions

To ensure the complete elution of the target analyte from the adsorbent, desorption conditions should be studied (Table 1). According to results for effect of pH, the adsorption of TC was not efficient in the acidic mediums. Therefore, elution with acidic solution may be more favorable. As a result, different concentrations (1–3 mol L^{-1}) of various acids and base were employed to reuse the adsorbent. From the data given in Table 1, it is obvious that 2.0 mL of 2.0 mol L^{-1} nitric acid could accomplish the quantitative elution of TC from the MoS_2. The effect of desorption time of the analyte from the adsorbent after elution was also studied. It was found that 5 min was adequate for the complete recovery of the analyte from the adsorbent. The relatively long desorption time may be attributed to the functional groups sensitive to pH in the antibiotic.

3.2.5. The effect of sample volume

To determine low concentrations of analyte in the sample, a high preconcentration factor is required for solid-phase extraction by using high sample volume. Different volumes of sample solution (10–100 mL) were used to study the effect of sample volume on the recoveries of analyte keeping other conditions constant. As shown in Fig. 2(B), quantitative recoveries were achieved for sample volumes up to 80 mL for TC. When sample volume is increased, the concentration of TC is decreased. The preconcentration factor in this method was 40 which are calculated by the ratio of the optimum sample volume to the eluent volume.

3.2.6. Effect of salinity

Addition of inorganic salt may cause a modification of interaction between TC and adsorbent. In the research, some salts including potassium carbonate (K_2CO_3), ammonium sulfate ($(NH_4)_2SO_4$), dipotassium hydrogen phosphate (K_2HPO_4), and NaCl were used. It was found that inorganic salts can help in the recovery of TC. When NaCl was added in the system, a clearer and more stable interface was formed. Therefore, NaCl was chosen. The effect of NaCl amount in the range of 0%–30.0% (w/v) was also investigated. The results were shown in Fig. 2(C). Taken as a whole, the general trend was evident and represented promotion effect. The percentage of recovery increased to the addition of NaCl and after 20% (w/v) NaCl reached an almost constant value.

The change of recovery with the addition of salt might result from the different contribution electrostatic interaction and of hydrophobic effect. The general improvement effect with the addition of NaCl might mainly owing to the well-known salting out effect [46]. With NaCl added, the solubility of TC in water decreased and the decrease in solubility facilitated the diffusion of more TC to the surfaces of the adsorbent and increases adsorption capabilities. So the hydrophobic effect might be predominant in the adsorption. For pH 4.5, the adsorption increased monotonically with increasing Na^+, which was probably due to the fact that TC mainly existed as zwitterions at pH 4.5 and this zwitterions form made it hardly have electrostatic interactions with MoS_2. It was thus deduced that besides hydrophobic effect, the electrostatic interactions between the analyte and MoS_2 also played a certain important role in the adsorption process.

3.2.7. Effect of interferences

The effects of the different foreign species were discussed in the determination of the concentration of TC. For this purpose, the described preconcentration method was applied for the model solutions of 20 mL containing 200 μg L^{-1} TC and interfering species added at different concentrations. With a relative error of less than ±5%, the tolerance limits for various foreign substances were listed in Table 2 (tolerance ratio in mass). The results showed that the recovery values for TC were obtained as ≥96% even in the presence of the following interferers: 10 mg L^{-1} spiramycin, gentamicin, chlortetracycline, oxytetracycline, prometryn, and atrazine. The results indicated that the majority of these foreign substances had no remarkable interference on the TC determination in the various water samples used in this work.

Table 1
Desorption of TC from surfaces of MoS_2 adsorbent under the influence of various eluents

Eluent	Concentration (mol L^{-1})	Volume (mL)	Recovery (%)
HNO_3	1	2	81.9 (2.7)
		1	72.6 (2.9)
	2	2	99.5 (2.7)
		4	98.2 (2.6)
	3	2	93.0 (2.8)
HCl	1	2	68.4 (3.5)
	2	2	84.7 (2.8)
NaOH	1	2	44.4 (3.1)
	2	2	58.2 (2.6)

Conditions: C_0: 200 μg L^{-1} of TC solution; mass of adsorbent: 10 mg; volume: 20 mL; contact time: 40 min; and desorption time: 5 min.

Table 2
Tolerance limits for substrates in adsorption of 200.0 μg L^{-1} of TC

Interference	Tested substrates to analyte ratio (w/w)	Recovery (%)
Spiramycin	50	100.6 (1.7)
Gentamicin	50	99.3 (1.6)
Chlortetracycline	50	102.7 (1.9)
Oxytetracycline	50	96.8 (2.8)
Prometryn	50	98.9 (2.9)
Atrazine	50	98.7 (3.1)

Conditions: Mass of adsorbent: 10 mg; volume: 20 mL; contact time: 40 min; and the washing conditions: 2 mL HNO_3 (2 mol L^{-1}).

3.3. Reusability of MoS_2 adsorbent

Reusability is a key feature regarding the evaluation performance of the adsorbent materials. The stability and reusability of the MoS_2 were assessed through the performance of five consecutive cycles of adsorption/desorption under the optimized conditions. The results of Fig. 3 showed that the MoS_2 was stable and reusable in the operation process (87%–95%) without any significant loss of capacity and decrease in the recovery of the studied target analyte.

3.4. Kinetic study

The experimental kinetic data of TC adsorption were correlated by pseudo-first-order, pseudo-second-order, intraparticle diffusion, and Elovich models to study the rate and mechanism of adsorption. The experimental adsorption data at initial TC concentration of 5 mg L^{-1} using 10 mg of MoS_2 adsorbent were examined and experimental data are presented in Table 3. These models can be represented with the following linear forms:

$$\log(q_e - q_t) = \log q_e - \frac{k_1}{2.303}t \quad (1)$$

$$\frac{t}{q_t} = \frac{1}{k_2 q_e^2} + \frac{1}{q_e}t \quad (2)$$

$$q_t = k_i t^{1/2} + C \quad (3)$$

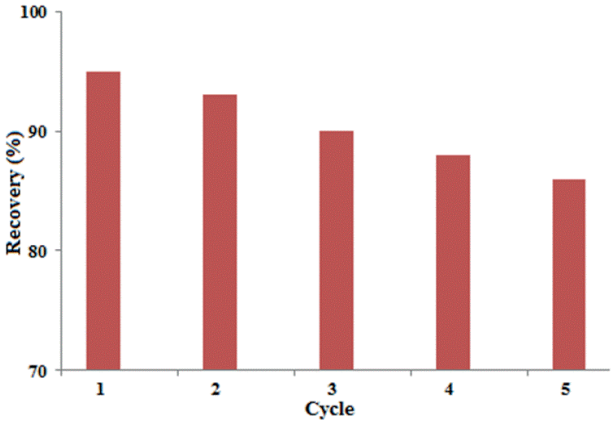

Fig. 3. Reusability cycle of TC adsorption using MoS_2 nanosheets. Conditions: C_0: 200 μg L^{-1} of TC solution; pH: 4.5; mass of adsorbent: 10 mg; volume: 20 mL; ionic strength: 20% w/v; and contact time: 60 min.

$$q_t = \frac{1}{\beta}\ln(\alpha\beta) + \frac{1}{\beta}\ln t \quad (4)$$

In the pseudo-first-order model [47] plotting the values of log $(q_e - q_t)$ vs. t may give a linear relationship. K_1 and q_e values were determined from the slope and intercept, respectively (Fig. 4(A)). Distance of intercept from experimental q_e value indicates that this model was not suitable for fitting the experimental data. In pseudo-second-order kinetic model [48], the plot of t/q_t vs. t gives a straight line with high correlation coefficient. Constant K_2 and equilibrium adsorption capacity (q_e) were calculated from the intercept and slope of this line, respectively (Fig. 4(B)). The high values of R^2 (0.99) strongly confirms the applicability of this model for explanation of adsorption kinetic data.

The intraparticle diffusion model relates between adsorption rate and square root of time (t) [49]. The values of K_{diff} and C were calculated from the slope and intercept of the plot of q_t vs. $t^{1/2}$. C value is related to the thickness of the boundary layer and K_{diff} is the intraparticle diffusion rate constant (mg g^{-1} $min^{-1/2}$) were obtained from the final linear portion of above mention plot and presented in Table 3. Since, the intraparticle curve did not pass through the origin (Fig. 4(C)); one can notice that in addition to the intraparticle diffusion model another stage such as second-order kinetic model controls the adsorption process. The Elovich equation as another rate equation based on the adsorption capacity in linear form was applied for the adsorption of the antibiotic from an aqueous medium [50]. The plot of q_t vs. ln(t) should yield a linear relationship with a slope and intercept of (1/β) and (1/β) ln(α β), respectively. The Elovich constants obtained from the slope and the intercept of the straight line (Fig. 4(D)) are reported in Table 3. It is observed that the adsorption of TC followed more closely to pseudo-second-order kinetics with regression coefficients >0.99 which fits the experimental data better than the other kinetic models for the entire adsorption process.

3.5. Adsorption isotherms

The absorption spectra of TC solution (5.0 mg L^{-1}), TC supernatant solution (0.89 mg L^{-1}) after adsorption 82% it on the adsorbent and MoS_2 alone are shown in Fig. 5. It can be seen that the spectrum of MoS_2 has no strong adsorption capacity above 270 nm, while it displays two adsorption peaks at 275 and 357 nm for TC. Also, it is clear that peak of TC at 357 has dropped in the analyte supernatant solution after adsorption. The results illustrated that TC successfully adsorbed on MoS_2 nanosheets surfaces.

Adsorption capacity is a key parameter for the evaluation of adsorbent, because it determines how much adsorbent is

Table 3
Adsorption kinetics constants of TC on MoS_2 nanosheets

Pseudo-first-order			Pseudo-second-order			Intraparticle			Elovich			
q_e^{cal} (mg g^{-1})	K_1 (min^{-1})	R^2	q_e^{cal} (mg g^{-1})	K_2 (g mg^{-1} min^{-1})	R^2	K_{id} (mg g^{-1} $min^{-1/2}$)	C	R^2	α (mg g^{-1} min^{-1})	β (g mg^{-1})	R^2	q_{exp} (mg g^{-1})
15.28	0.04	0.81	13.64	0.001	0.99	98.58	1.93	0.95	18.80	0.37	0.87	13.25

Conditions: Concentration: 5 mg L^{-1}; volume: 20 mL; ionic strength: 20% w/v; and adsorbent: 10 mg.

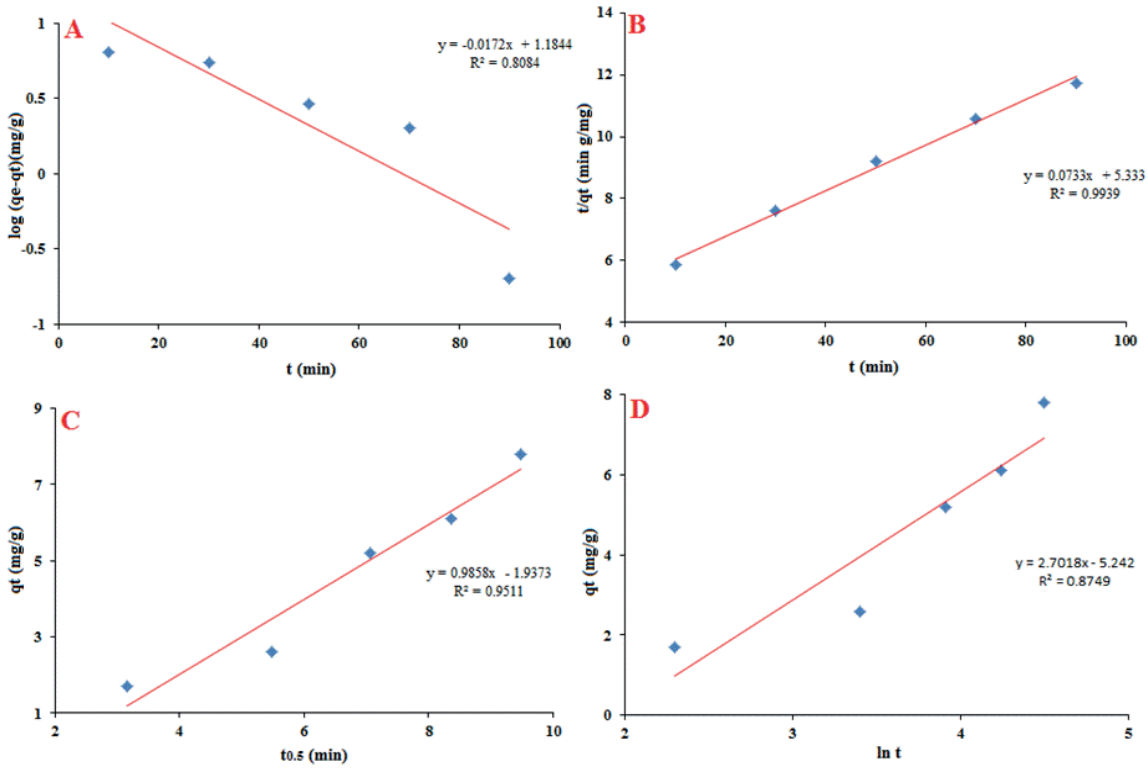

Fig. 4. Kinetic plots for adsorption of TC on MoS_2 nanosheets. (A) Pseudo-first-order plot, (B) pseudo-second-order plot, (C) intraparticle plot, and (D) Elovich plot. Conditions: C_0: 5 mg L^{-1} of TC solution; pH: 4.5; mass of adsorbent: 10 mg; volume: 20 mL; ionic strength: 20% w/v; and at the temperature of 303 K.

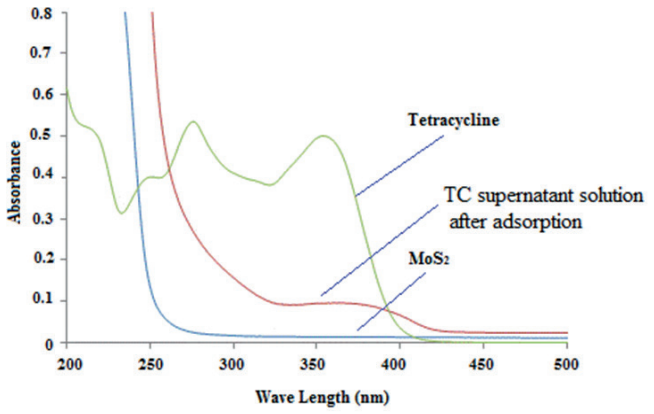

Fig. 5. The UV–vis absorption spectra of tetracycline, tetracycline adsorbed on MoS_2 nanosheets, and MoS_2. Conditions: C_0: 5 mg L^{-1} of TC solution; pH: 4.5; mass of adsorbent: 10 mg; volume: 20 mL; ionic strength: 20% w/v; and contact time: 40 min.

required for quantitative enrichment of the analyte from a given solution [51]. In order to gain a better understanding of adsorption mechanisms and evaluate the adsorption performance, the experimental data for TC adsorption onto MoS_2 nanosheets are analyzed using the Langmuir and Freundlich adsorption isotherm models. The pH of model solutions of 20 mL containing 5–100 mg L^{-1} of TC was adjusted to 4.5 and was added to 10.0 mg adsorbent. The mixture was centrifuged, after shaking for 60 min. 2.0 mL of the eluted of solution with eluent was analyzed by UV–vis.

The adsorption data were fitted according to the linear form of the Langmuir isotherm model based on the following equation [52]:

$$\frac{C_e}{q_e} = \left(\frac{1}{K_L q_m}\right) + \left(\frac{C_e}{q_m}\right) \quad (5)$$

where q_e (mg g^{-1}) is the equilibrium adsorption capacity, q_{max} (mg g^{-1}) is the maximum amount of adsorbed analytes per unit weight of adsorbent to form complete monolayer coverage on the surface, C_e (mg L^{-1}) is the equilibrium concentration of analyte in aqueous solution, and K_L (L mg^{-1}) represents enthalpy of sorption.

The Freundlich isotherm model represents properly the sorption process at low or intermediate concentration of analytes on a heterogeneous surface. It has the following equation:

$$q_e = K_F . C_e^{1/n} \quad (6)$$

where K_F (mg^{1-n} L^n g^{-1}) and n are the Freundlich constant related to the adsorption capacity and adsorption intensity, respectively. The adsorption data were fitted according to the linear form of the Freundlich isotherm model.

Adsorption isotherm parameters of Langmuir and Freundlich models for the adsorption of the TC on the MoS_2 nanosheets at 303 K are listed in Table 4. The adsorption isotherm fitted Langmuir model better than Freundlich model due to the larger correlation coefficient (R^2), suggesting that TC adsorption on MoS_2 is monolayer chemical adsorption process.

Langmuir isotherm was used to determine the q_e and K_L values from the linear coefficients obtained by plotting C_e/q_e as a function of C_e. The adsorption capacity was found to be 57.47 mg g^{-1}. The Langmuir constant was 0.0182 L mg^{-1}.

3.6. Adsorption thermodynamic

The influence of temperature on TC adsorption was also conducted under different temperature from 283 to 313 K. As shown in Fig. 2(D), the temperature varying from 283 to 313 K had little impact on the adsorption of TC.

The thermodynamic parameters were evaluated to confirm the nature of the adsorption and the inherent energetic changes involved during TC adsorption. Standard enthalpy ($\Delta H°$), free energy ($\Delta G°$), and entropy change ($\Delta S°$) were calculated to determine the thermodynamic feasibility and the spontaneous nature of the process. Therefore, the values of $\Delta H°$ and $\Delta S°$ were obtained from the slope and intercept of the $\ln K_d$ vs. $1/T$ curve according to Eq. (7):

$$\ln K_d = \left(\frac{\Delta S°}{R}\right) - \left(\frac{\Delta H°}{RT}\right) \quad (7)$$

while the $\Delta G°$ value can be determined from:

$$\Delta G = \Delta H° - T\Delta S° \quad (8)$$

where K_d (L g^{-1}) is the distribution coefficient ($K_d = q_e/C_e$), T (K) is the adsorption temperature, and R (8.314 J mol^{-1} K^{-1}) is the universal gas constant.

As shown in Table 5, the value of $\Delta G°$ for TC adsorption was negative at all temperatures, indicating that the adsorption of TC onto MoS_2 was spontaneous and thermodynamically feasible. The observed positive $\Delta H°$ and $\Delta S°$ values for TC adsorption suggested an endothermic process and increasing the temperature promoted the interaction between TC molecules and MoS_2.

Table 4
Adsorption isotherms parameters of Langmuir and Freundlich models for the adsorption of the TC on MoS_2 nanosheets adsorbent

Langmuir			Freundlich		
K_L (L mg^{-1})	q_{max} (mg g^{-1})	R^2	K_F	$1/n$	R^2
0.018	57.47	0.997	1.450	0.696	0.992

Conditions: Volume: 20 mL; pH: 4.5; contact time: 60 min; adsorbent: 10 mg; and concentration: 5–100 mg L^{-1}.

Table 5
Thermodynamic parameters for TC adsorption on MoS_2 nanosheets

Thermodynamic parameters	283 K	293 K	303 K	313 K
$\Delta G°$ (kJ/mol)	–0.670	–0.614	–0.438	–0.312
$\Delta H°$ (kJ/mol)	0.199			
$\Delta S°$ (J/mol K)	0.324			

Conditions: Volume: 20 mL; ionic strength: 20% w/v; contact time: 60 min; adsorbent: 10 mg; and concentration: 10 mg L^{-1}.

3.7. Evolution of the method performance

3.7.1. Analytical performance of the method

The analytical characteristics of the proposed SPE method based on MoS_2 adsorbent were investigated. A calibration curve was constructed by preconcentration of 20 mL of sample standard solutions under the optimum experimental conditions described above. The calibration curve for TC was high level of linearity in the range of 0.025–5 mg L^{-1} with the equation $y = 0.65x + 0.0047$. A good correlation coefficient ($R^2 = 0.993$) was obtained. The detection limit (LOD = 3 SB/m) and limit of quantifications (LOQ = 10 SB/m) based on seven times the standard deviation of the blank determined 7.91 and 24.35 μg L^{-1}, respectively. The relative standard deviation (RSD, %) for seven replicate measurements of 200 μg L^{-1} TC was 3.3%.

3.7.2. Analytical application

For accessing the capability of the method for different samples, the method was applied to preconcentration and

Table 6
Determination results for TC in water samples

Real sample	Spiked (μg L^{-1})	Founded[a] (μg L^{-1})	R (%)	Measurement by HPLC (μg L^{-1})
Fish pond water[b]	0	185.2 ± 1.99	–	187.2 ± 1.99
	50.0	233.4 ± 1.02	96	237.2 ± 1.02
Agriculture-influenced water[b]	0	124 ± 2.03	–	130.4 ± 2.03
	50.0	176.8 ± 2.56	102	174.7 ± 2.56
River water[b]	20.0	22.62 ± 0.33	103	25.62 ± 0.33
	50.0	47.21 ± 1.41	94	51.21 ± 1.41

Conditions: Volume: 20 mL; adsorbent: 10 mg; ionic strength: 20% w/v; contact time: 60 min, washing conditions: 2 mL HNO_3 (2 mol L^{-1}).
[a]Mean value ± standard deviation based on three replicate measurements.
[b]Fom Var e olia village, Mahallat, Iran.

Table 7
Comparison of our proposed method with others methods of preconcentration of TC

Sorbent	Linear range (mg L^{-1})	LOD (μg L^{-1})	LOQ (μg L^{-1})	RSD (%)	Ref.
Discovery DSC-phenyl	0.05–0.65	4	–	1.2	[53]
MIP monolithic column	0.05–10	16.1	–	3.8	[54]
Silica-coated magnetite particles	0.03–0.6	0.01	–	2.1	[55]
Phenyl-silica	0.26–248	53	–	2.1	[56]
MoS_2 nanosheets	0.025–5	7.91	24.35	3.3	This work

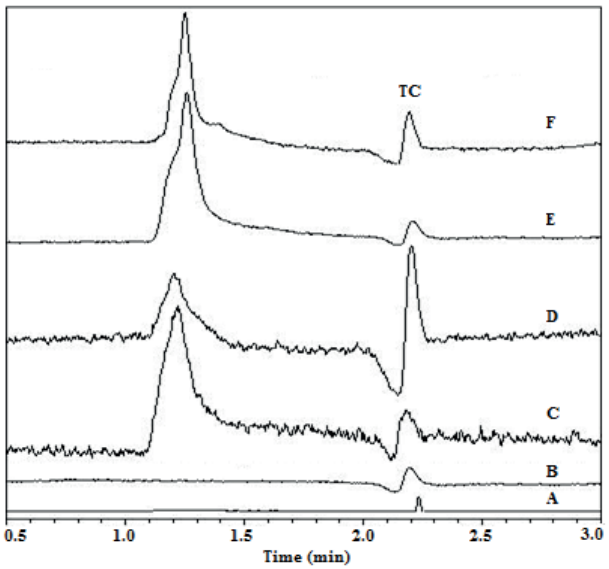

Fig. 6. HPLC chromatogram of the water samples after the extraction under the optimized conditions by the proposed method. (A) River water spiked with 20 μg L^{-1} and (B) 50 μg L^{-1}, (C) non-spiked fish pond water and (D) 50 μg L^{-1} spiked of TC, and (E) non-spiked agriculture-influenced water and (F) 50 μg L^{-1} spiked of TC.

determination of TC from 20 mL from the fish pond water, agriculture-influenced water, and river water. The results were summarized in Table 6. As can be seen, the recovery values for TC were changed from 92.0% to 103.0% at optimum conditions (20 mL sample volume pH 4.5, 10 mg MoS_2 as adsorbent, 60 min as adsorption time, 2 mL of 2 mol L^{-1} HNO_3 as eluent, and 5 min as desorption time). These results show that the developed method can be applied for water samples. The *t*-test method was used to do a significant difference test for proposed method and HPLC ($P = 0.95$, $f = 3$). The results were found in Table 6 and Fig. 6. It was found that the data of both methods did not have significant difference and the analytical results were in good agreement with the certified values.

3.7.3. Comparison of our proposed method with others

The proposed method with MoS_2 nanoadsorbent was compared with several used sorbent (Table 7). Our proposed low cost preconcentration system shows good adsorption with reasonable preconcentration and analysis time and comparable with other preconcentration methods and also its LOD for proposed method is comparable to those given by other reported work. The results of our work were obtained by inexpensive UV–vis instrument. The most important feature of our proposed adsorbent was that MoS_2 nanosheet would not undergo any pretreatment step and was synthesized simply. This novel and effective method requires low eluent volume (2 mL) and it can also be successfully applied to real samples.

4. Conclusion

In this study, for the first time MoS_2 nanosheet was applied for preconcentration of TC antibiotic as an example of polycyclic aromatic compounds in solid-phase extraction. This adsorbent adsorbs polycyclic aromatic compounds by π–π stacking. The main advantage of MoS_2 was its needless character to modification or functionalization, simple synthesis, reusability, environmentally friendly, and numerous adsorption sites in edges and surfaces in order to improve adsorption capacity. The Langmuir equation fitted the adsorption isotherm well. In conclusion, the proposed method reveals the great potential of MoS_2 as an advantageous adsorbent material in SPE. Although the obtained results of this research were related to the TC preconcentration, the system could be a considerable potential guide for the preconcentration and determination of other polycyclic aromatic compounds which are environmental pollutants.

Acknowledgment

Support of this investigation by the Research Council of University of Tehran through grants is gratefully acknowledged.

References

[1] L. Ji, F. Liu, Z. Xu, S. Zheng, D. Zhu, Adsorption of pharmaceutical antibiotics on template-synthesized ordered micro- and mesoporous carbons, Environ. Sci. Technol., 44 (2010) 3116–3122.
[2] H. Sun, X. Shi, J. Mao, D. Zhu, Tetracycline sorption to coal and soil humic acids: an examination of humic structural heterogeneity, Environ. Toxicol. Chem., 29 (2010) 1934–1942.
[3] S. Thiele-Bruhn, Pharmaceutical antibiotic compounds in soils – a review, J. Plant Nutr. Soil Sci., 166 (2003) 145–167.
[4] Z. Li, L. Schulz, C. Ackley, N. Fenske, Adsorption of tetracycline on kaolinite with pH-dependent surface charges, J. Colloid Interface Sci., 351 (2010) 254–260.
[5] S. Boleas, C. Alonso, J. Pro, C. Fernández, G. Carbonell, J.V. Tarazona, Toxicity of the antimicrobial oxytetracycline to soil organisms in a multi-species-soil system (MS 3) and influence of manure co-addition, J. Hazard. Mater. 122 (2005) 233–241.

[6] S. Thiele-Bruhn, I.-C. Beck, Effects of sulfonamide and tetracycline antibiotics on soil microbial activity and microbial biomass, Chemosphere, 59 (2005) 457–465.
[7] B. Halling-Sørensen, Inhibition of aerobic growth and nitrification of bacteria in sewage sludge by antibacterial agents, Arch. Environ. Contam. Toxicol., 40 (2001) 451–460.
[8] L. Ji, W. Chen, J. Bi, S. Zheng, Z. Xu, D. Zhu, et al., Adsorption of tetracycline on single-walled and multi-walled carbon nanotubes as affected by aqueous solution chemistry, Environ. Toxicol. Chem., 29 (2010) 2713–2719.
[9] N. Furusawa, Isolation of tetracyclines in milk using a solid-phase extracting column and water eluent, Talanta, 59 (2003) 155–159.
[10] M.A. Rudek, C.L. March, K.S. Bauer, J.M. Pluda, W.D. Figg, High-performance liquid chromatography with mass spectrometry detection for quantitating COL-3, a chemically modified tetracycline, in human plasma, J. Pharm. Biomed. Anal., 22 (2000) 1003–1014.
[11] L. Monser, F. Darghouth, Rapid liquid chromatographic method for simultaneous determination of tetracyclines antibiotics and 6-epi-doxycycline in pharmaceutical products using porous graphitic carbon column, J. Pharm. Biomed. Anal., 23 (2000) 353–362.
[12] Y. Wang, X. Xu, J. Han, Y. Yan, Separation/enrichment of trace tetracycline antibiotics in water by [Bmim] BF4–$(NH_4)_2SO_4$ aqueous two-phase solvent sublation, Desalination, 266 (2011) 114–118.
[13] P.-H. Chang, Z. Li, T.-L. Yu, S. Munkhbayer, T.-H. Kuo, Y.-C. Hung, et al., Sorptive removal of tetracycline from water by palygorskite, J. Hazard. Mater., 165 (2009) 148–155.
[14] L. Zhang, X. Song, X. Liu, L. Yang, F. Pan, J. Lv, Studies on the removal of tetracycline by multi-walled carbon nanotubes, Chem. Eng. J., 178 (2011) 26–33.
[15] C. Gu, K.G. Karthikeyan, Interaction of tetracycline with aluminum and iron hydrous oxides, Environ. Sci. Technol., 39 (2005) 2660–2667.
[16] Y. Gao, Y. Li, L. Zhang, H. Huang, J. Hu, S.M. Shah, et al., Adsorption and removal of tetracycline antibiotics from aqueous solution by graphene oxide, J. Colloid Interface Sci., 368 (2012) 540–546.
[17] I. Turku, T. Sainio, E. Paatero, Thermodynamics of tetracycline adsorption on silica, Environ. Chem. Lett., 5 (2007) 225–228.
[18] Z. Li, P.-H. Chang, J.-S. Jean, W.-T. Jiang, C.-J. Wang, Interaction between tetracycline and smectite in aqueous solution, J. Colloid Interface Sci., 341 (2010) 311–319.
[19] Y.-J. Wang, D.-A. Jia, R.-J. Sun, H.-W. Zhu, D.-M. Zhou, Adsorption and cosorption of tetracycline and copper (II) on montmorillonite as affected by solution pH, Environ. Sci. Technol., 42 (2008) 3254–3259.
[20] A. Caroni, C.R.M. De Lima, M.R. Pereira, J.L.C. Fonseca, The kinetics of adsorption of tetracycline on chitosan particles, J. Colloid Interface Sci., 340 (2009) 182–191.
[21] W.-R. Chen, C.-H. Huang, Adsorption and transformation of tetracycline antibiotics with aluminum oxide, Chemosphere, 79 (2010) 779–785.
[22] K.-J. Choi, S.-G. Kim, S.-H. Kim, Removal of antibiotics by coagulation and granular activated carbon filtration, J. Hazard. Mater., 151 (2008) 38–43.
[23] Y. Chao, W. Zhu, F. Chen, P. Wang, Z. Da, X. Wu, et al., Commercial diatomite for adsorption of tetracycline antibiotic from aqueous solution, Sep. Sci. Technol., 49 (2014) 2221–2227.
[24] Y. Chao, W. Zhu, B. Yan, Y. Lin, S. Xun, H. Ji, et al., Macroporous polystyrene resins as adsorbents for the removal of tetracycline antibiotics from an aquatic environment, J. Appl. Polym. Sci., 131 (2014).
[25] Y. Chao, W. Zhu, J. Chen, P. Wu, X. Wu, H. Li, et al., Development of novel graphene-like layered hexagonal boron nitride for adsorptive removal of antibiotic gatifloxacin from aqueous solution, Green Chem. Lett. Rev., 7 (2014) 330–336.
[26] Y. Chao, W. Zhu, Z. Ye, P. Wu, N. Wei, X. Wu, et al., Preparation of metal ions impregnated polystyrene resins for adsorption of antibiotics contaminants in aquatic environment, J. Appl. Polym. Sci., 132 (2015).
[27] J.-M. Lv, Y.-L. Ma, X. Chang, S.-B. Fan, Removal and removing mechanism of tetracycline residue from aqueous solution by using Cu-13X, Chem. Eng. J., 273 (2015) 247–253.
[28] M. Sánchez-Polo, I. Velo-Gala, J.J. López-Peñalver, J. Rivera-Utrilla, Molecular imprinted polymer to remove tetracycline from aqueous solutions, Microporous Mesoporous Mater., 203 (2015) 32–40.
[29] M. Hershfinkel, L.A. Gheber, V. Volterra, J.L. Hutchison, L. Margulis, R. Tenne, Nested polyhedra of MX2 (M = W, Mo; X = S, Se) probed by high-resolution electron microscopy and scanning tunneling microscopy, J. Am. Chem. Soc., 116 (1994) 1914–1917.
[30] F. Schwierz, Nanoelectronics: flat transistors get off the ground, Nat. Nanotechnol., 6 (2011) 135–136.
[31] E. Benavente, M.A. Santa Ana, F. Mendizábal, G. González, Intercalation chemistry of molybdenum disulfide, Coord. Chem. Rev., 224 (2002) 87–109.
[32] R. Lv, H. Terrones, A.L. Elías, N. Perea-López, H.R. Gutiérrez, E. Cruz-Silva, et al., Two-dimensional transition metal dichalcogenides: clusters, ribbons, sheets and more, Nano Today, 10 (2015) 559–592.
[33] B. Radisavljevic, A. Radenovic, J. Brivio, V. Giacometti, A. Kis, Single-layer MoS_2 transistors, Nat. Nanotechnol., 6 (2011) 147–150.
[34] H. Hwang, H. Kim, J. Cho, MoS_2 nanoplates consisting of disordered graphene-like layers for high rate lithium battery anode materials, Nano Lett., 11 (2011) 4826–4830.
[35] H. Li, G. Lu, Z. Yin, Q. He, H. Li, Q. Zhang, et al., Optical identification of single- and few-layer MoS_2 sheets, Small, 8 (2012) 682–686.
[36] M. Pumera, A.H. Loo, Layered transition-metal dichalcogenides (MoS_2 and WS_2) for sensing and biosensing, TrAC, Trends Anal. Chem., 61 (2014) 49–53.
[37] M. Komarneni, A. Sand, U. Burghaus, Adsorption of thiophene on inorganic MoS_2 fullerene-like nanoparticles, Catal. Lett., 129 (2009) 66–70.
[38] Y. Chao, W. Zhu, X. Wu, F. Hou, S. Xun, P. Wu, et al., Application of graphene-like layered molybdenum disulfide and its excellent adsorption behavior for doxycycline antibiotic, Chem. Eng. J., 243 (2014) 60–67.
[39] H. Song, S. You, X. Jia, Synthesis of fungus-like MoS_2 nanosheets with ultrafast adsorption capacities toward organic dyes, Appl. Phys. A., 121 (2015) 541–548.
[40] V.G. Pol, S.V. Pol, A. Gedanken, Micro to nano conversion: a one-step, environmentally friendly, solid state, bulk fabrication of WS_2 and MoS_2 nanoplates, Cryst. Growth Des., 8 (2008) 1126–1132.
[41] H.S.S. Ramakrishna Matte, A. Gomathi, A.K. Manna, D.J. Late, R. Datta, S.K. Pati, et al., MoS_2 and WS_2 analogues of graphene, Angew. Chem. Int. Ed., 122 (2010) 4153–4156.
[42] R.S. Hixson, J.N. Fritz, Shock compression of tungsten and molybdenum, J. Appl. Phys., 71 (1992) 1721–1728.
[43] X. Van Doorslaer, K. Demeestere, P.M. Heynderickx, H. Van Langenhove, J. Dewulf, UV-A and UV-C induced photolytic and photocatalytic degradation of aqueous ciprofloxacin and moxifloxacin: reaction kinetics and role of adsorption, Appl. Catal., B, 101 (2011) 540–547.
[44] B. Li, T. Zhang, Removal mechanisms and kinetics of trace tetracycline by two types of activated sludge treating freshwater sewage and saline sewage, Environ. Sci. Pollut. Res., 20 (2013) 3024–3033.
[45] Y. Tang, H. Guo, L. Xiao, S. Yu, N. Gao, Y. Wang, Synthesis of reduced graphene oxide/magnetite composites and investigation of their adsorption performance of fluoroquinolone antibiotics, Colloids Surf., A, 424 (2013) 74–80.
[46] W. Yang, Y. Lu, F. Zheng, X. Xue, N. Li, D. Liu, Adsorption behavior and mechanisms of norfloxacin onto porous resins and carbon nanotube, Chem. Eng. J., 179 (2012) 112–118.
[47] S. Lagergren, About the theory of so-called adsorption of soluble substances, (1898).
[48] Y.-S. Ho, G. McKay, Pseudo-second order model for sorption processes, Process Biochem., 34 (1999) 451–465.

[49] W.J. Weber, J.C. Morris, Kinetics of adsorption on carbon from solution, J. Sanit. Eng. Div., 89 (1963) 31–60.
[50] S.H. Chien, W.R. Clayton, Application of Elovich equation to the kinetics of phosphate release and sorption in soils, Soil Sci. Soc. Am. J., 44 (1980) 265–268.
[51] H. Tavallali, H. Malekzadeh, M.A. Karimi, M. Payehghadr, G. Deilamy-Rad, M. Tabandeh, Chemically modified multiwalled carbon nanotubes as efficient and selective sorbent for separation and preconcentration of trace amount of Co(II), Cd(II), Pb(II), and Pd(II), Arabian J. Chem., (2014).
[52] E. Yavuz, S. Tokaliouglu, H. Sahan, S. Patat, Ultralayered Co_3O_4 as a new adsorbent for preconcentration of Pb(II) from water, food, sediment and tobacco samples, Talanta, 115 (2013) 724–729.